

Comparison of photoluminescence properties of Zn-and O-polar ZnO thin films

R. TÜLEK*, M. PARLAK, A. TEKE

Department of Physics, Faculty of Science and Letter, Balikesir University, Balikesir, Turkey

Optical properties of Zn- and O-polar Zinc Oxide (ZnO) thin films grown by molecular beam epitaxy (MBE) were investigated by the temperature and excitation intensity dependent photoluminescence (PL) measurements. The behavior of excitonic transitions and the transitions originating from the deep-level defect centers were studied in detail. It was observed that the peak energy value of the transition, which dominates the low-temperature (10K) PL spectra for both samples, belonged to the neural donor-bound exciton (DOXA) centered at about 3.362 eV. The peak energy of the free exciton (FXA) transition for both samples was observed at 3.376 eV and 3.28 eV at low temperature and room temperature, respectively, with a total redshift of approximately 96 meV, which is compatible with the Varshni equation. On the other hand, the maximum band edge emission (DOXA) peak intensity of Zn-polar sample was approximately 2.5 times higher than of O-polar sample. At room temperature, where the free exciton transition (FXA) is dominant, this ratio drops to 1.8 times. The temperature behaviors of the band edge emission peak intensities were determined by fitting an empirical relation assuming two thermally activated nonradiative centers with different activation energy and trapping rates. It was observed that the excitation power density dependence of the PL densities follows a power law of $I \propto P^k$, where k power factor was found close to one for both samples. The ratios of green luminescence peak intensities of the excitonic transition were also compared in the respective excitation intensity range.

(Received May 24, 2023; accepted October 6, 2023)

Keywords: ZnO, Photoluminescence, Zn-polar, O-polar

1. Introduction

Due to its some unique properties such as direct band gap (3.3 eV at 300 K), a large exciton binding energy (60 meV), wide crystal-growth technology, ZnO has great potential for various optoelectronic and microelectronic applications such as light emitting diodes, UV photodetectors, short wavelength lasers, field emission devices, gas sensors [1-5]. ZnO has the wurtzite structure with a lack of inversion symmetry, which induces different polar surfaces along the c-axis, like Zn-polar (0001) and O-polar (000 $\bar{1}$) faces [6]. Zn-polar and O-polar faces of ZnO exhibit different physical properties which plays an important role in electronic/optoelectronic device performance [7]. Therefore, various studies have been carried out in the literature to reveal the relationship between the optical properties and surface polarities of bulk, thin film or nanostructured ZnO [6-16]. In some of these studies, it was reported that the Zn-polar and O-polar faces showed extremely different emission characteristics from PL measurements [6-10]. From the literature, different mechanisms, such as exciton-phonon coupling strength, opposite band bending, adsorbed molecules and surface states, defect centers, have been proposed as the source of the observed differences in PL properties of Zn-polar and O-polar-faced samples [6,7,9,11].

In this paper, we examined and compared the optical properties of MBE grown Zn-polar and O-polar Zinc Oxide (ZnO) thin films by the temperature and excitation intensity dependent PL measurements. Temperature-

dependent measurements were performed in the temperature range of 10- 300 K and excitation intensity dependent measurements at 10K were performed in the range of 2.6-330 mW/cm². The behaviors of excitonic transitions and the transitions originating from the deep-level defect centers were studied and compared in detail.

2. Results and discussions

The samples were grown on c-plane sapphire substrate by MBE. In photoluminescence measurements, the samples were excited with a 349 nm frequency triple Nd: YLFQ switched pulse laser, dispersed with a 500 mm spectrometer using 1200 lines/mm grating, and detected with Concentrated Charge Coupled Device (ICCD) camera. In the temperature-dependent measurements, the driving current of the laser was held constant at 1.3 A, corresponding to an excitation intensity of 13 mW/cm². Fig. 1(a and b) shows the temperature dependent PL spectra of samples taken in temperatures range of 10-300 K. As seen in Fig. 1 the temperature dependent PL spectra for both samples exhibit similar behavior in general. At low temperature, spectra are dominated by band-edge free and bound excitonic transitions, while the intensity of these transitions decreases rapidly as the temperature increases. Comparison of band edge emission of PL spectra taken at 10K is enlarged in Fig. 1(c). As seen from this figure there is no significant difference in the peak positions of the band-edge transitions. The peaks observed

at 3.376 eV as a shoulder on the high energy side of the main peak in the band edge emission region of both samples belong to the A free exciton (FXA). The transitions dominating the band edge emission region observed at a peak energy of 3.362 eV correspond to the neutral donor-bound exciton (D0XA). The peak observed

at about 3.332 eV belongs to the donor-acceptor-pair (DAP) transition. The shoulder seen at approximately 3.26 eV, which is redshifted at 72 meV, are the first longitudinal optical phonon [1-LO (DAP)] replicas of DAP. The peak intensity of the 1-LO copy is 5.4 times lower than the peak intensity of the main transition.

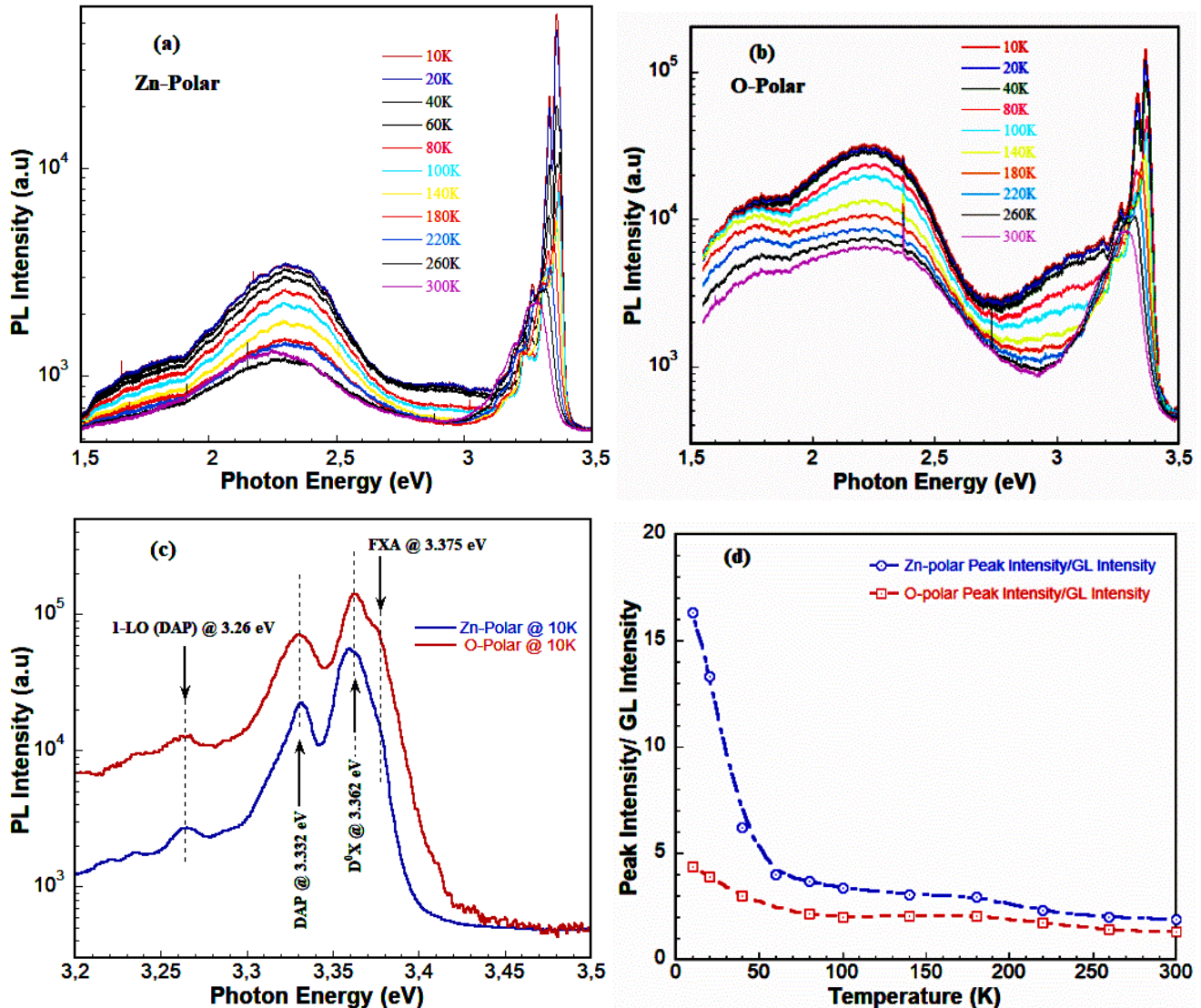


Fig. 1. PL spectra of (a) Zn-polar (b) O-polar samples taken in the temperature range of 10-300K. (c) Comparison of band edge emission region of 10K PL spectra of Zn-polar and O-polar samples. (d) Temperature-dependent variation of the ratio of band edge emission peak intensity to green luminescence peak intensity of samples (color online)

Due to the lattice expansion and electron-phonon interaction strength that increases with increasing temperature, the free exciton peaks for both samples are redshifted at about 96 meV and centered at 3.28 eV at room temperature. The temperature-dependent variation is well characterized by the Varshni equation [17] using fitting parameters consistent with the literature [14]. As seen in Fig. 1 (a) and (b), no significant temperature-dependent variation in the peak positions of the transitions associated with deep level defects was observed. In both samples, blue luminescence (BL) and red luminescence (RL) peaks were observed at approximately 2.90 eV and

1.78 eV, respectively. A slight difference is observed between the Zn- and O-polar samples in green luminescence (GL). The origin of these transitions has been widely discussed in the literature with various arguments [18-26]. The GL transition observed at 2.32 eV in the Zn-polar sample was observed at a peak energy of 2.24 eV in the O-polar sample. This 8 meV shift in the peak position may be due to the difference in the strength of the phonon interaction with the defect centers considered as the source of the GL transitions. Another interpretation can be made that the yellow luminescence (YL) transition, which cannot be clearly resolved due to

the wide line width of the GL transition, is more dominant in the O-polar sample.

The PL intensity gradually decreases as the temperature increases, either due to thermal activation of non-radiative centers or thermal escape of carriers involved in the emission process. The temperature behavior of the band edge emission peak intensity is determined by an empirical equation assuming two thermally activated nonradiative centers with different activation energy and trapping rates. For both samples, the PL intensities decrease at relatively small rates at low temperatures, but more gradually at higher temperatures. This indicates that there are two nonradiative recombination centers that are responsible for low- and high-temperature regimes. The thermal activation energies and the corresponding capture rates for the low and high temperature regime are extracted by fitting the dual channel Arrhenius equation [27]. Low temperature activation energies of 6.7 meV, and 5 meV with capture rate constants of 12 and 3, and high temperature activation energies of 37.6 meV and 37.8 meV with capture rate of 55 were obtained for Zn- and O-polar samples, respectively.

Another important parameter in the comparison of the optical properties of Zn-polar and O-polar samples is the temperature-dependent variation of the ratio of band edge emission peak intensity to deep level defect-related green luminescence peak intensity. In Fig. 1 (d), temperature-dependent variation of the ratio of dominant band edge emission peak intensity to green luminescence peak intensity of both samples are given. As seen in the figure, this ratio is approximately 16.3 and 4.4 times at low temperature for Zn- and O-polar samples, respectively. As the temperature rises to 60K, it drops very quickly down to about 4 times in the Zn-polar sample. On the other hand, this ratio drops to only 2.5 times for the O-polar sample in the same temperature range. This difference between Zn- and O-polar samples can be attributed to their low temperature non-radiative activation energies and corresponding capture rates. As discussed above, the ratio of non-radiative activation energies and their capture rates, which is about 2.9 times between two samples, is consistent with this result. As the temperature increases further, the density ratio decreases at a very slow rate for both samples (even with small peak in the 150-200K

temperature range) due to the less decay rate of the free exciton compared to donor-bound excitons. Therefore, free exciton (FXA) transition becomes the dominant band edge emission at higher temperatures. As the temperature increases, the difference in this intensity ratio decreases and becomes 1.9 and 1.3 times for Zn- and O-polar samples, respectively, at room temperature. From these analyses, it can be argued that the density of the defect centers is higher in the O-polar sample than in the Zn-polar sample.

PL measurements based on excitation intensity were made in gradual increments between the lowest (2.6 mW/cm²) and the highest (330 mW/cm²) values at 10 K. Excitation intensity dependent PL spectra for Zn-polar and O-polar samples are given in Fig. 2. As seen in Fig. 2, the samples exhibit similar characteristic behavior. The line widths of the emission band in the excitonic region of both samples increase with increasing excitation intensity due to exciton-phonon interactions. At moderate excitation intensity, interactions such as double-exciton, exciton-exciton and exciton-carrier can have significant effects on the characteristics of the spectrum. As the excitation intensity increases further, electron-hole pair formation can occur by breaking the exciton-exciton bonds [28]. In the current study, the excitation intensity range is low to medium. The comparison of photoluminescence spectra measured at maximum excitation intensity for Zn-polar and O-polar samples is shown in the inset of Fig. 2 (b). From figure the peak position of the band edge transition is redshifted by 8 meV in both samples. In the deep level defect-related transition regions of the spectrum, no shifts in BL peak positions were observed, but shifts in GL peak positions occurred for Zn- and O-polar samples. It is seen that the GL peak position of the Zn-polar sample is centered at about 2.27 eV with a 5 meV redshift, and the GL peak position of the O-polar sample is centered at 2.36 eV with a 12 meV blue shift. The reason for this behavior is unclear, but the yellow luminescence transition is likely to be within the broad line width of GL band. The redshift of the GL band of the Zn-polar sample with increasing excitation intensity may be due to the increase in YL intensity. Conversely, the blue shift of the GL peak energy value in the O-polar sample can be explained by the decrease in YL intensity.

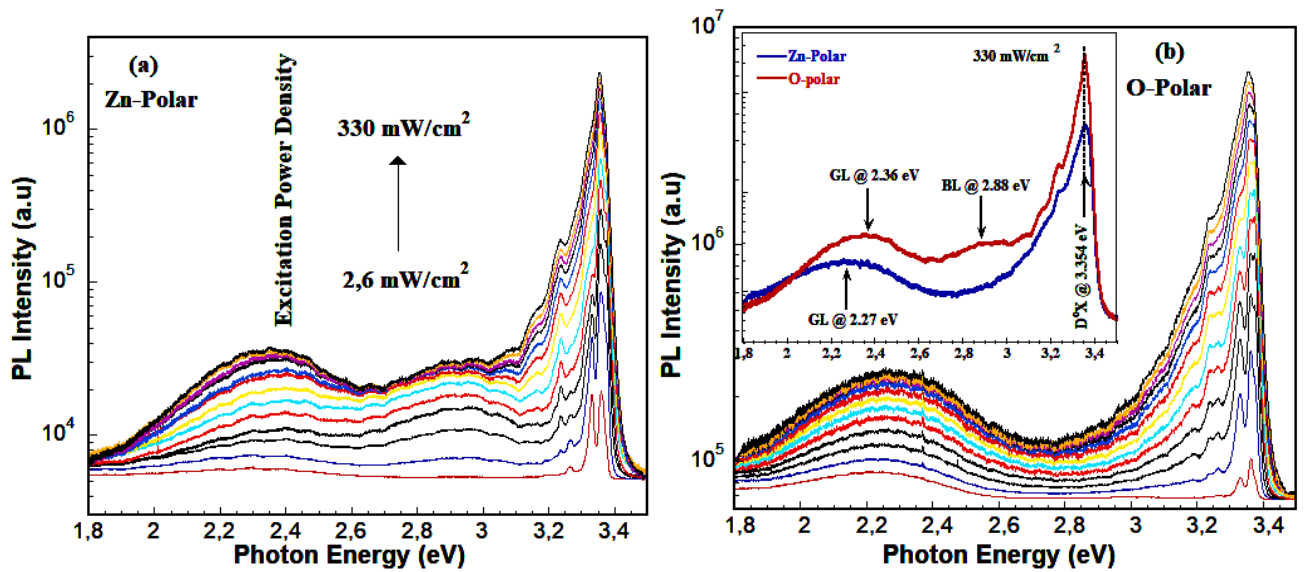


Fig. 2. The PL spectra of (a) Zn-polar ve (b) O-polar samples taken in the excitation power density range of 2.6-330 mW/cm² at 10 K. (b) inset shows, the comparison of photoluminescence spectra measured at maximum excitation power density for Zn-polar and O-polar samples (color online)

The behavior of luminescence intensity on excitation power is used to characterize excitonic, donor-acceptor-pair (DAP) and free-bound (FB)-like transitions. In general, it is found that the luminescence intensity I follows a power law in the form of $I \propto P^k$ where k is the power coefficient and P is excitation power [29].

The power factor k is a parameter that depends on the nature of recombination. Since the density of state of the

defect centers is limited, the intensities of the defect-related transitions are expected to be saturated at high excitation intensities. Therefore, $k > 1$ indicates the dominance of excitonic transitions, and $k < 1$ indicates the dominance of free-bound, donor-acceptor pair and defect-related transitions [29, 30].

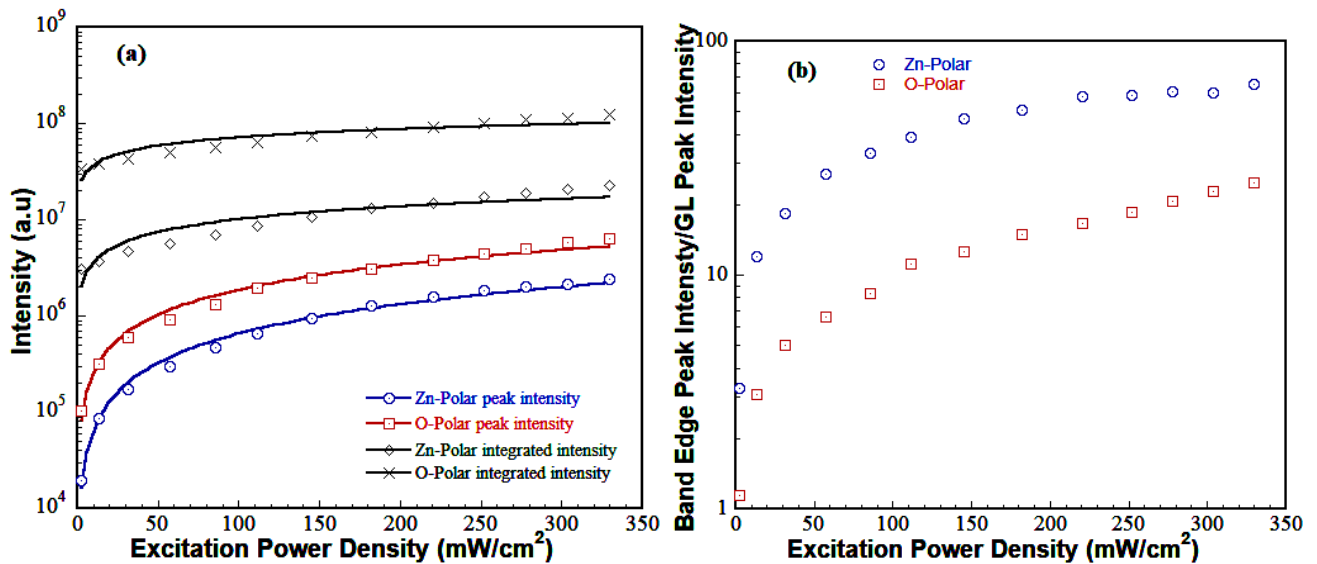


Fig. 3. (a) Variation of band edge emission peak intensity depending on excitation power density for Zn-polar and O-polar samples (b) Variation of the ratio of the band edge peak intensity to GL intensity with excitation power density (color online)

According to the best fit to the power law in the current excitation intensity range, the peak intensity of band edge emission increases approximately linearly, as expected, with the excitation power density in both samples

($k = 1$ for Zn – polar and $k = 0.9$ for O – polar). On the other hand, the k values of the integrated intensities are much smaller than one and are found to be $k = 0.4$ and $k = 0.3$ for the Zn-polar and O-polar samples, indicating that the defect densities are high in both samples. Fig. 3

(b) shows the ratio of band edge peak intensity to GL intensity varies with excitation intensity. It increases at the same rate in both samples. At the lowest excitation intensity, this ratio was approximately 3.3 and 1.2 times, while at the highest excitation intensity, it was found 66 and 25 times in Zn-polar and O-polar samples, respectively.

3. Conclusions

The temperature and excitation power density dependent photoluminescence measurements were performed to determine optical properties of Zn- and O-polar ZnO thin films grown on c-sapphire substrates. For both samples, it was observed that band edge emission is dominated by neutral donor-bound exciton transition centered at about 3.362 eV at 10K PL spectrum. The peaks correspond to A free exciton (FXA) transition were observed at 3.376 eV and 3.28 eV at 10K and 300K, respectively. A total redshift of approximately 96 meV was found to be consistent with Varshni equation. The temperature behavior of the band edge peak intensity was analyzed by using dual-channel Arrhenius equation. The thermal activation energies and corresponding rate constants for low and high temperature regime were deduced. Although the thermal activation energies and corresponding capture rates are the same for both samples at the high temperature region, the decrease of peak intensity in Zn-polar sample is about 3 times faster than that of O-polar sample at the low temperature regime. The excitation power density dependence of the band edge peak intensities, total integrated intensities, and the ratios of the peak intensities of the excitonic transition to the green luminescence were investigated using the power law. The power factors k were determined to be close to one for the band edge peak intensities for both samples. It was found to be much less than one for the total integrated intensities. The ratio of excitonic emission peak intensities to defect-centered green luminescence peak intensities versus excitation power density follow the same rate for both samples. This ratio is 2.7 times higher in the Zn-polar sample than in the O-polar sample. From the temperature and excitation intensity dependent analyses, it can be concluded that density of the defect centers is lower in Zn-polar sample than O-polar sample, resulting in better optical properties.

Acknowledgments

Authors thank Hadis MORKOÇ, Ümit ÖZGÜR and Vitaliy Avrutin from Virginia Commonwealth University for providing the samples used in this study and valuable suggestions on manuscript.

References

[1] A. Teke, Ü. Özgür, S. Doğan, X. Gu, H. Morkoç,

- B. Nemeth, J. Nause, H. O. Everitt, *Phys. Rev. B* **70**, 195207 (2004).
- [2] W. Lin, R. Ma, J. Xue, B. Kang, *Sol. Energy Mater. Sol. Cells* **91**, 1902 (2007).
- [3] H. J. Lim, D. Yong, Y. J. Oha, *Sensors and Actuators A* **125**, 405 (2006).
- [4] N. O. Korsunska, L. V. Borkovska, B. M. Bulakh, L. Yu. Khomenkova, V. I. Kushnirenko, I. V. Markevich, *J. of Luminescence* **102-103**, 733 (2003).
- [5] C. G. van de Walle, *Physica B: Condensed Matter* **308**, 899 (2001).
- [6] D. C. Oh, T. Kato, H. Goto, S. H. Park, T. Hanada, T. Yao, J. J. Kim, *Appl. Phys. Lett.* **93**, 241907 (2008).
- [7] S. Lautenschlaeger, J. Sann, N. Volbers, B. K. Meyer, A. Hoffmann, U. Haboeck, M. R. Wagner, *Phys. Rev. B* **77**, 144108 (2008).
- [8] R. E. Sherriff, D. C. Reynolds, D. C. Look, B. Jogai, J. E. Hoelscher, T. C. Collins, G. Cantwell, W. C. Harsch, *J. Appl. Phys.* **88**(6), 3454 (2000).
- [9] S. A. Chevtchenko, J. C. Moore, Ü. Özgür, X. Gu, A. A. Baski, H. Morkoç, B. Nemeth, J. E. Nause, *Appl. Phys. Lett.* **89**, 182111 (2006).
- [10] M. W. Allen, P. Miller, R. J. Reeves, S. M. Durbin, *Appl. Phys. Lett.* **90**, 062104 (2007).
- [11] A. Yamamoto, Y. Moriwaki, K. Hattori, H. Yanagi, *Appl. Phys. Lett.* **98**, 061907 (2011).
- [12] C. Luo, M. A. Rahman, M. R. Phillips, C. Ton-That, M. Butterling, A. Wagner, F. Chi-Chung Ling, *Thin Solid Films* **711**, 138303 (2020).
- [13] C. J. Youn, T. S. Jeong, M. S. Han, J. H. Kim, *J. Crystal Growth* **261**(4), 526 (2004).
- [14] H. Sasaki, H. Kato, F. Izumida, H. Endo, K. Maeda, M. Ikeda, Y. Kashiwaba, I. Niikura, Y. Kashiwaba, *Phys. Stat. Sol. C* **3**, 4 (2006).
- [15] S. Lautenschlaeger, J. Sann, N. Volbers, B. K. Meyer, A. Hoffmann, U. Haboeck, M. R. Wagner, *Phys. Rev. B* **77**, 144108 (2008).
- [16] D. C. Oh, T. Kato, H. Goto, S. H. Park, T. Hanada, T. Yao, J. J. Kim, *Appl. Phys. Lett.* **93**, 241907 (2008).
- [17] Y. P. Varshni, *Physica* **34**, 149 (1967).
- [18] K. M. Johansen, L. Vines, T. S. Bjorheim, R. Schifano, B. G. Svensson, *Phys. Rev. Appl.* **3**, 024003 (2015).
- [19] D. C. Look, K. D. Leedy, L. Vines, B. G. Svensson, A. Zubiaga, F. Tuomisto, D. R. Doutt, L.J. Brillson, *Phys. Rev. B* **84**, 115202 (2011).
- [20] M. D. McCluskey, S. J. Jokela, *J. Appl. Phys.* **106**, 071101 (2009).
- [21] A. Janotti, C. G. van de Walle, *Phys. Rev. B* **76**, 165202 (2007).
- [22] F. Tuomisto, V. Ranki, K. Saarinen, D. C. Look, *Phys. Rev. Lett.* **91**, 205502, (2003).
- [23] B. Lin, Z. Fu, Y. Jia, *Appl. Phys. Lett.* **79**, 7 (2001).
- [24] Z. Wang, C. Luo, W. Anwand, A. Wagner, M. Butterling, M. A. Rahman, M.R. Phillips, C. Ton-That, M. Younas, S. Su, F. C. Ling, *Sci. Rep.* **9**, 3534 (2019).

- [25] B. Panigrahy, M. Aslam, D. S. Misra, M. Ghosh, D. Bahadur, *Adv. Funct. Mater.* **20**, 7 (2010).
- [26] M. S. Wang, Y. Zhou, Y. Zhang, E. J. Kim, S. H. Hahn, S. G. Seong, *Appl. Phys. Lett.* **100**, 10 (2012).
- [27] J. Y. Park, J. H. Lee, S. Jung, and T. Ji, *Phys. Status Solidi A* **213**, 1610 (2016).
- [28] Ü. Özgür, Ya. I. Alivov, C. Liu, A. Teke, M. A. Reshchikov, S. Doğan, V. Avrutin, S.-J. Cho, H. Morkoç, *J. Appl. Phys.* **98**, 041301 (2005).
- [29] T. Schmidt, G. Daniel, K. Lischka, *J. Cryst. Growth* **117**(1), 748 (1992).
- [30] Younghun Hwang, Youngho Um, Hyoyeol Park, *J. of the Korean Phys. Society* **58**, 5 (2011).

*Corresponding author: baran265@gmail.com;
baran@balikesir.edu.tr